Journal of Applied Polymer Science

Preparation and characterization of poly(glycerol sebacate)/cellulose nanocrystals elastomeric composites

Ling Zhou, Hui He, Can Jiang, Shuai He
College of Materials Science and Engineering, South China University of Technology, Guangzhou, China
Correspondence to: H. He (E-mail: pshuihe@scut.edu.cn)

ABSTRACT: Poly(glycerol sebacate) (PGS) is one of the new elastomers used for soft tissue engineering, while improving its limited mechanical strength is the biggest challenge. In this work, a novel biodegradable elastomer composite PGS/cellulose nanocrystals (CNCs) was prepared by solution-casting method and the mechanical properties, sol–gel contents, crosslink density, and hydrophilic performance were characterized. The thermal and degradation properties of composites were also investigated. Results show that the addition of CNCs into PGS resulted a significant improvement in tensile strength and modulus, as well as the crosslink density and the hydrophilicity of PGS. When the CNCs loading reached 4 wt %, the tensile strength and modulus of the composite reached 1.5 MPa and 1.9 MPa, respectively, resulting 204% and 158% increase compared to the pure PGS. Prolonging the curing time also improved the strength of both the neat PGS and PGS/CNCs composites according to the association and shift of hydroxy peaks around 3480 cm^{-1}. DSC results indicate that the addition of CNCs improved both the crystallization capacity and moving capability of PGS molecular chain. © 2015 Wiley Periodicals, Inc. J. Appl. Polym. Sci. **2015**, *132*, 42196.

KEYWORDS: biodegradable; biopolymers and renewable polymers; composites; mechanical properties; polyesters

Received 23 December 2014; accepted 9 March 2015
DOI: 10.1002/app.42196

INTRODUCTION

Novel materials, which have physical, mechanical, and chemical properties similar to those found *in vivo*, provide a potential platform in building artificial microenvironments for tissue engineering and therapeutic applications.[1] Despite huge efforts having been invested into the development of synthetic biomaterials since 1990s, currently there are few synthetic products available for practical clinical use that can substitute the soft, mechanically functional tissues such as muscle and connective tissue.[2] Over the past 10 years, there has been an increasing research activity towards the development and application of synthetic biodegradable polyester elastomers (e.g., PGS,[3–6] poly(polyol sebacate),[7] and polycaprolactone)[8] as transplantable biomaterials for tissue engineering.

PGS, a remarkable biodegradable elastomer with attractive properties, is the most well studied.[9] It exhibits a covalently crosslinked three-dimensional molecular structure that provides thermoset elastomeric properties. As a promising elastomer which primarily focus on soft tissue engineering applications such as cardiac muscle, vascular tissue engineering, cartilage, nerve conduits, and retina etc., PGS has several advantages like relatively inexpensive, good biocompatibility, tunable degradation property, and bioresorbability which means the degradation products of PGS could be absorbed in the body and ultimately be removed via natural metabolic processes.[10–12]

However, the mechanical properties of PGS are only controllable within a narrow range, which are tailored by altering the curing time and curing temperature. The Young's modulus (YM) and ultimate tensile strength (UTS) of PGS fluctuated between 0.05∼1.45 MPa and 0.05∼0.6MPa, respectively.[13,14] It is useful for substituting some particular types of tissue, such as muscle (YM at 0.01–0.5 MPa), vascular tissue (YM at 0.05–1 MPa) etc., but except for some others like skin or tendon. An effective and simple method to improve the mechanical properties of PGS is to prepare PGS-based nanocomposites by loading some inorganic reinforcing nano-fillers, such as Bioactive glasses particles,[9] nanosilica,[15] halloysite nanotubes,[16] and Carbon nanotubes[17] etc., which has been reported a lot recent years. For instance, Chen *et al.*[16] reported the average values of Young's modulus (E), ultimate tensile strength (UTS), and elongation at break (ξmax) of PGS/halloysite nanotubes were observed to improve with increasing halloysite additions, in which E increased from 0.80 to 1.51 MPa, UTS increased from 0.60 to 1.60 MPa, whilst ξmax increased from 110% to 225% with the addition of halloysite increased from 0 to 20 wt %.

CNCs, an abundant natural organic material, doubtlessly have attracted significant interest over the past 20 years.[18] It is commonly extracted by removing the amorphous phase from cellulose with hydrolysis under controlled acidic conditions.[19,20] The elastic modulus of CNCs is experimentally determined as 70−140 GP.[21] Due to their green sources, stiffness, and biocompatibility, CNCs have been considered as a reinforcement material for biopolymers, and the resulting biocomposites have been used as tissue scaffolds.[22] Compared to these inorganic nanofillers, the biodegradable CNCs performs better in improving mechanical properties with a lower loading as a bio-based reinforcing nano-filler.[18]

In this work, CNCs were added into PGS to develop a novel family of elastic bio-composites. The primary objective was to prepare, characterize, and evaluate the properties of PGS/CNCs composites and investigate the reinforcement mechanism of these newly developed bio-composite materials. The morphological and structural characteristics of isolated CNCs and PGS/CNCs composites were analyzed through TEM and SEM, respectively. Tensile test, FTIR spectroscopy, sol–gel test, and DSC were performed to characterize the changes of mechanical, componential, and thermal properties in composites. *In vitro* degradation behavior of PGS/CNCs composites was also tested.

EXPERIMENTAL

Materials

Raw cotton stalk fibers were supplied by Shanxi Gerui Equipment Co. Ltd (China), which was grinded and then passed through 80 meshes (less than 0.178 mm size screen). Sebacic acid (SA) (purity > 99.5%) was obtained from the Sinopharm Chemical Reagent Co. Ltd of Shanghai. Glycerol (purity > 99.0%) and tetrahydrofuran (THF) was purchased from Fuyu Fine Chemical Institute of Tianjin. Other chemical reagents used for isolating CNCs like sodium hydroxide, sodium chlorite, hydrogen peroxide, acetic acid, absolute ethyl alcohol, and sulfuric acid were all purchased from Fuyu Fine Chemical Institute of Tianjin in China. All the chemicals were reagent grade and used as received.

Extraction of CNCs

The dried cotton stalk powders were first alkali treated by soaking into 12.5 w/w % NaOH solution at 160°C for 2 h, followed by washing with adequate distilled water to remove most of the hemicelluloses and lignin. Then the dried and ground cotton cellulose was bleached with 1% (w/v) sodium chlorite solution (fiber to liquor ratio of 1 : 30) at 75°C for 1 h with an acetate buffer to maintain the solution pH < 4. This procedure was repeated twice to remove the residual lignin. Finally, the cotton stalk CNCs were extracted by acid hydrolysis with 64 wt % sulfuric acid at 45°C for 45 min with vigorous stirring. After being quenched by adding 10 fold deionized water, the suspension was centrifuged at 9000 rpm for 15 min to remove the excess of aqueous acid and to concentrate the cellulose crystals. The resultant precipitate was rinsed and redispersed in absolute ethyl alcohol, then recentrifuged. After being washed with absolute ethyl alcohol twice, the CNCs were suspended in another 120 ml absolute ethyl alcohol again and ultrasonic dispersed for 15 min. The CNCs content of the suspension was calculated by weighing the CNCs in a certain volume of suspension after drying.

Preparation of PGS/CNCs Composites

The PGS and composites were prepared in two stages. Initially a PGS prepolymer was synthesized by polycondensation of 1 : 1 molar ratio of the glycerol (purity 99%) and the sebacic acid (purity 99%) at 130°C for 24 h under nitrogen gas with mechanical agitation.[23] The reaction was incomplete while the pre-polymer was still ungelled and could be dissolved in ethyl alcohol. Different percentages (0, 1, 2, 3, and 4 wt %) of CNCs was mixed with a 50 wt % solution of PGS pre-polymer in ethyl alcohol solution and magnetically stirred for 30 min at ambient temperature. The slurry was then cast onto a Teflon mold with the ethyl alcohol evaporated at 60°C to produce ~1 mm thick sheet of PGS/CNCs composite. Finally the cast sheet was further polymerized at 130°C for an additional 48 h under vacuum to obtain the final materials.

Characterization Studies

The microstructure and morphology of CNCs were visualized by a Hitachi H-7650 transmission electron microscope at an accelerating voltage of 80 kV. The samples for TEM measurement were prepared by dropping the sample solution on Cu grids of 200 meshes.

Morphologies of PGS/CNCs composites with 0 and 2 wt % CNCs were observed by Nova Nano SEM 430 instrument (FEI, Netherlands) under an acceleration voltage of 10 kV. SEM specimens were prepared by fracturing the composites in liquid nitrogen and were coated with gold before examination.

FTIR spectra were recorded in attenuated total reflection (ATR) mode with a Bruker Vertex 70 FTIR spectrometer at a spectral resolution of 4 cm^{-1} and 32 scans. The surfaces of film samples were cleaned by absolute ethanol before tested.

Tensile tests were performed at room temperature with an Instron 5560 mechanical tester equipped with an 100 N load cell, and at a cross-head speed of 10 mm/min. Dog-bone shaped specimens of 25 mm × 4 mm × t mm (t = thickness) were punched out from sheet material, using a standard mode.

The sol–gel contents and Degree of Swelling (DS) of PGS in THF aimed to determine the crosslink density of PGS. Briefly, dried, pre-weighed (M_0) samples were swollen in the THF until no weight gain was observed. The specimens were considered to be fully swollen and the mass of the equilibrium swollen network (M_{eq}) was determined. Then the samples were dried in a vacuum oven at 40°C for 3 days and weighed again to determine the mass of the dried network (M_d). The Gel content was calculated as the ratio of the mass of the dried extracted polymer to the measured dry mass of the elastomer:

$$W_{Gel}(\%) = \frac{(Md - M0 * wt.\%CNCs)}{M0(1 - wt.\%CNCs)} * 100,\ W_{sol}(\%) = 100\text{-}W_{Gel} \quad (1)$$

The DS was calculated as:

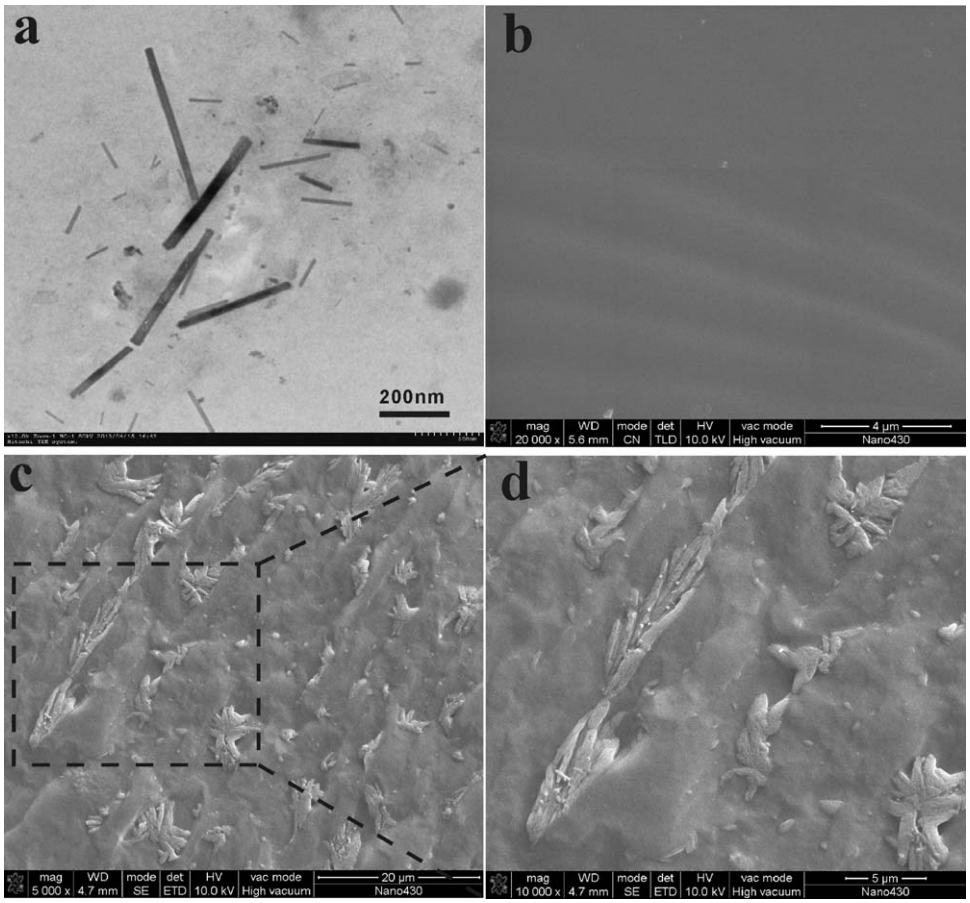

Figure 1. TEM image of cotton stalks CNCs (a) and SEM images of neat PGS (b) and PGS with 2 wt % CNCs (c, d).

$$\frac{(\mathrm{Meq}-\mathrm{Mcnc})-(\mathrm{Md}-\mathrm{Mcnc})}{\mathrm{Md}-\mathrm{Mcnc}}=\frac{\mathrm{Meq}-\mathrm{Md}}{\mathrm{Md}(1-\mathrm{wt.\%CNCs})}*100\% \quad (2)$$

The Water Contact angle of samples and water absorption of gel were also tested to determine the hydrophilic performance of the composite. Water contact angle was tested by DSA100 contact angle meter (KRUSS, Germany). The water absorption ability was measured by weighing the weights of Gel (1.5 mm in thickness and 10 mm in diameter) before (M_{Gel}) and after (M_{nGel}) soaking in water by 48 h.

$$W_{water}=\frac{\mathrm{MnGel}-\mathrm{MGel}}{\mathrm{MGel}}*100\% \quad (3)$$

The thermal stabilities of PGS/CNCs were characterized using a thermogravimetric analyzer (TA Instruments Q2000, USA). The amount of sample for each measurement was about 5∼8 mg. All of the measurements were performed under a nitrogen atmosphere with a gas flow of 20 ml/min and heated up to 700°C at a heating rate of 20°C/min.

In vitro degradation of the composites was tested in PBS solution (PH≈7.4) at 37±1°C. The small disc samples (1.5 mm in thickness and 10 mm in diameter) were used for the *in vitro* degradation study of the composites in PBS solution. A sample of weight G_1 was put into a taper bottle and immersed in PBS solution (20 mL) at 37 ± 1°C. The PBS solution was replaced every 4 days. After certain degradation time, the sample was taken out and completely dried to weight G_2. The mass loss was calculated according to the formula of $(G_1–G_2)/G_1\times100\%$. Two specimens were tested for obtaining average values.[17]

RESULT AND DISCUSSION

Microstructure of PGS/CNCs Composites

TEM image of CNCs from cotton stalks is shown in Figure 1(a), the dimensions of CNCs ranged from 10 to 50 nm in width and 100 to 300 nm in length. SEM images of the PGS and PGS/CNCs composite are also shown in Figure 1. For all images, the gray regions stood for the PGS matrixes, while the fiber bundles of various shapes which appeared both inside and outside of the PGS matrixes, represented the CNCs. Observed from Figure 1(c), most of the CNCs aggregations were uniformly distributed in sizes of several micrometers in the matrix, while other CNCs singles dispersed in nanoscale. As shown in Figure 1(d), it was found that the CNCs aggregations were formed by several rod-like CNCs singles, which meant that the CNCs tended to gather with themselves in PGS. This was probably due to three reasons: firstly, the compatibility between hydrophobic PGS matrix and hydrophilic CNCs was bad; secondly, the nano-scale CNCs have a tendency to aggregate themselves in order to reduce surface energy according to the typical

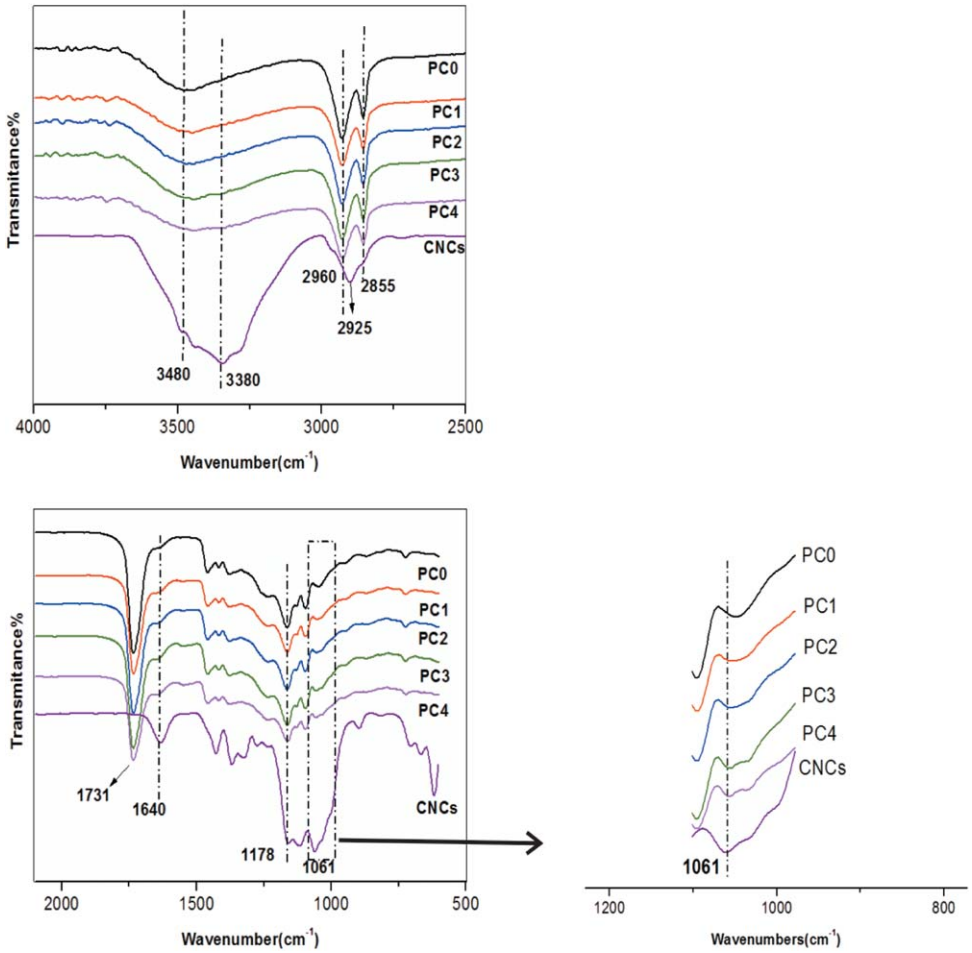

Figure 2. FITR curves of PGS (PC0), PGS/CNCs composites (PC1, PC2, PC3, PC4 represent PGS with 1, 2, 3, 4 wt % of CNCs respectively) and CNCs. [Color figure can be viewed in the online issue, which is available at wileyonlinelibrary.com.]

characteristic of nano-particles; thirdly, the strong intermolecular hydrogen-bond in CNCs also forced them to gather with each other. However, it was well-known that both the dispersion of CNCs in polymer matrixes and interfacial interactions between them are the key factors influencing the physical properties of the final composites. A homogeneous dispersion of CNCs and strong interfacial interactions between the PGS matrixes and CNCs can effectively improve the mechanical, electrical and thermal performances of the composites. In this case, how to disperse the CNCs in PGS matrix uniformly will be the key point for improving the mechanical strength of PGS/CNCs composites. This is also the next research target what we will focus on.

FTIR Spectra Analysis

FT-IR spectra of the PGS (PC0), PGS/CNCs composites (PC1, PC2, PC3, and PC4 represent PGS with 1, 2, 3, and 4 wt % of CNCs, respectively) and CNCs are shown in Figure 2. For PGS, the formation of ester bonds was indicated by the intense peak at 1731cm^{-1} and 1178 cm^{-1}, which represented the successful synthesis of PGS.[24] Simultaneously, it was noticed that all composites presented the similar absorption peaks and close absorption intensities with the matrix, indicating that CNCs did not change the main chemical structure of the PGS. The absorption peaks of the C–O–C at C_6 stretching vibrations in CNCs (corresponding to 1061 cm^{-1}) appeared in the composites evidenced the successful incorporation of CNCs into PGS. The two absorption peaks around 2925 cm^{-1} were attributed to the –CH_2 and –CH, respectively, and the broad peak observed around 3480 cm^{-1} was due to hydrogen bonds formed by hydroxyl groups. It was worth noting that the peak around 3480 cm^{-1} tended to be broad and shifted to low wavenumbers with increasing CNCs loadings, indicating the formation of a strong interaction between PGS and CNCs through hydrogen bonding (Scheme 1).[25]

Tensile Properties of PGS/CNCs Composites

Mechanical properties of the composite are always paid much attention and used to directly reflect the reinforcement effect of the fillers added.[17] PGS/CNCs composites showed typical stress–strain curves of elastomer at ambient temperature, as no stress whitening or plastic deformation were visually noticed [Figure 3(a)]. First, the tensile stress and modulus tended to be improved with the increase of CNCs loadings. When the CNCs loading reached 4 wt %, the strength and modulus of the composite increased from 0.45 MPa to 1.5 MPa and 0.76 MPa to

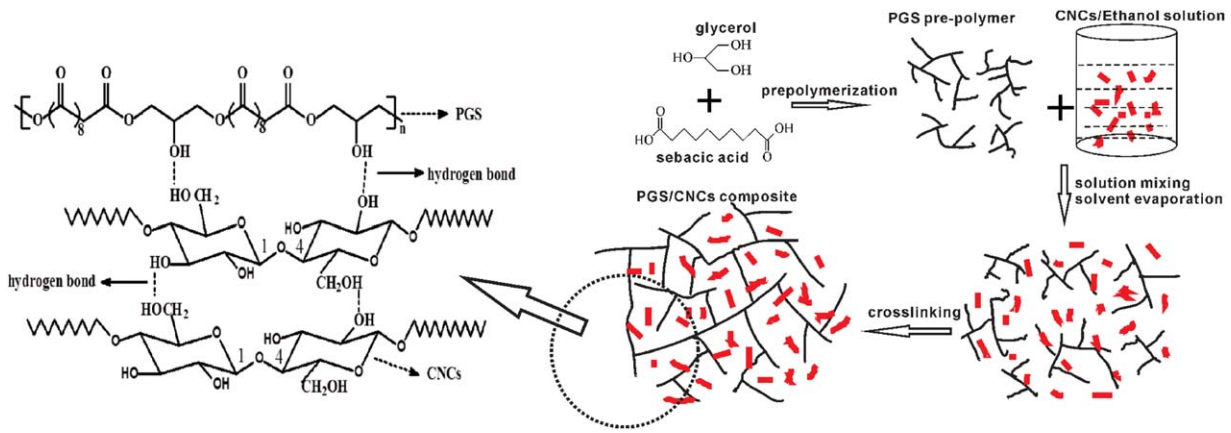

Scheme 1. Preparation of PGS/CNCs composites and Hydrogen-bond interaction between PGS and CNCs. [Color figure can be viewed in the online issue, which is available at wileyonlinelibrary.com.]

1.9 MPa, respectively, which increased by 204% and 158% compared to the pure PGS [Figure 3(b,c)]. This mechanical behavior was possibly attributed to: (1) high strength of CNCs itself as the filler; (2) hydrogen-bond interaction between the –OH of PGS and CNCs; and (3) the increase of crosslinking density of PGS (Table I) caused by the adding of CNCs. Meanwhile, the elastomeric nature of composites was due to both the crosslinking of PGS and the hydrogen bonding interactions between the hydroxyl groups of PGS and CNCs. As Figure 3(d) shown, the elongation at break of all composites was close to that of the pure PGS, which was different from the normal elastomeric behavior that the increase in strength and modulus was usually accompanied by the decrease in elongation at break. It means the reinforcement of PGS was achieved without compromising the extensibility of material.

Extensive researches indicate that the mechanical properties of PGS may be tailored by altering three processing parameters:

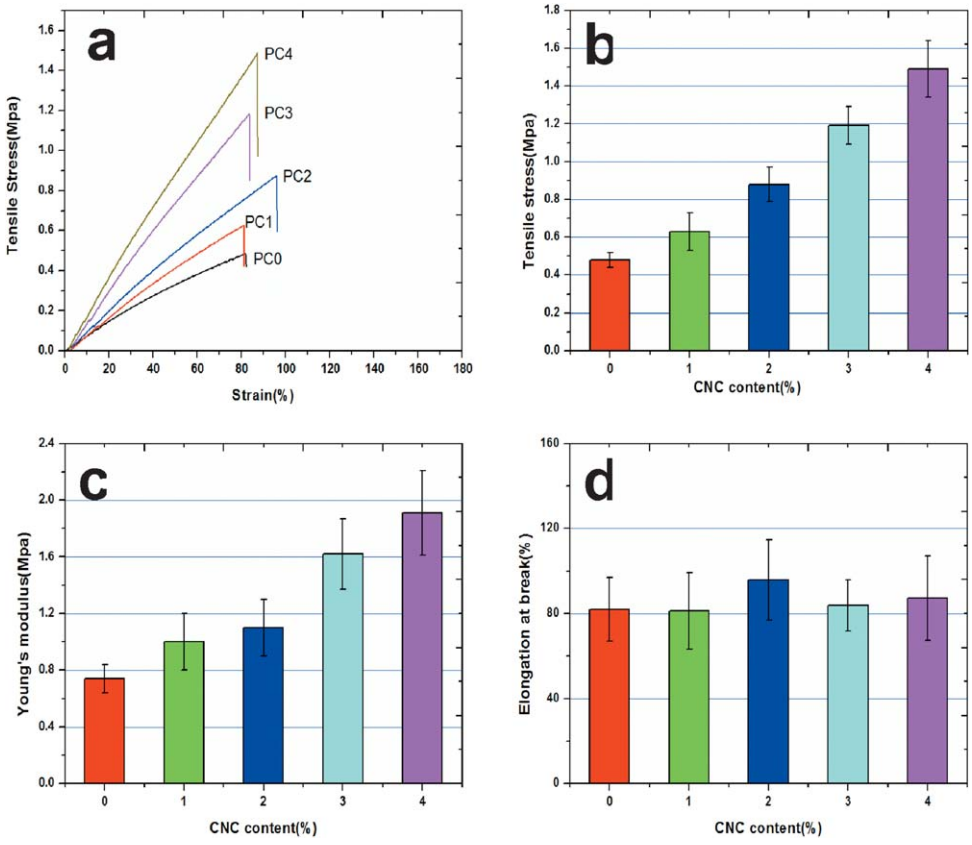

Figure 3. Tensile properties of PGS/CNCs composites: (a) Tensile stress–strain curves; (b) Tensile strength; (c) Tensile modulus; (d) Elongation at break. [Color figure can be viewed in the online issue, which is available at wileyonlinelibrary.com.]

Table I. The Tensile Properties of PC0 (Neat PGS) and PC2 at Different Crosslinking Curve Time

	PC0				PC2			
Curing time (hour)	36	48	60	72	36	48	60	72
Tensile strength (MPa)	0.23	0.37	0.62	0.74	0.57	0.87	1.25	1.63
Young's modulus (MPa)	0.18	0.43	1.42	2.05	0.61	1.28	2.26	3.04
Elongation at break (%)	168	116	53	42	121	87	70	68

(1) curing time, (2) molar ratio of glycerol to sebacic acid, and (3) curing temperature.[13,26,27] In this work, we chose the curing time as the variable to characterize whether the PGS (with or without CNCs) follow the same stress–strain behavior [Figure 4]. As it shown, when the neat PGS and PGS with 2 wt % CNCs (PC2) were crosslinked under different curing time (36∼72h), they still displayed similarly elastomer stress–strain curves. The average ultimate tensile stress and modulus of the PGS and PGS/CNCs both increased greatly with curing duration, whereas the strain at break decreased. This result was consistent with several previous researches,[14,28,29] which indicated that prolonged curing time gradually promoted the development of crosslinked network of PGS, subsequently improved the strength of materials. Therefore, the introduction of CNCs not only changed this tendency, but also strengthened it.

Sol–Gel Contents and Degree of Swelling (DS) of PGS/CNCs Composites

As it is reported by several researches, the synthesis of PGS elastomers is performed by two steps: (1) pre-polycondensation step which forms a PGS branched prepolymer (sol) and (2) crosslinking into a 3D net structure (gel) which offers flexibility and strength. Knowledge of the sol–gel and swelling behavior of the PGS elastomers is necessary for their applications. Table II shows that the sol fraction of PGS reduced from 21.2% to 13.2% and the gel contents increased accordingly with the increase of CNCs contents. It indicated that CNCs improved the crosslinking density of PGS. The similar conclusion was also proved by the increase of degree of swelling (DS) which greatly depended on the crosslinking density of PGS.[30] This result seemed to be the opposite to our previous thought that the adding of CNCs would hinder the further crosslinking, because it restricted the movement of PGS pre-polymer molecular chain with the increasing viscosity of mixture. One possible explanation was that the plentiful high activity hydroxyl (–OH) of cellulose could further esterify with the residual carboxylic acid groups of sebacic acid under high temperature and vacuum condition.

Hydrophilic Abilities of PGS/CNCs Composites

As shown in Table II and Figure 5(b,c), the water absorption of gel increased but the water contact angle of composites decreased with the increasing percentage of CNCs, which led to the conclusion that both the surface and interior of PGS/CNCs composites became increasingly hydrophilic. This was caused by the strong hydrophilic ability of CNCs whose surface contains abundant oxhydryl groups.

Thermal Behaviors of PGS/CNCs Composites

To investigate the effects of CNCs on the thermal behaviors of PGS matrix, the DSC study (Figure 6 and Table III) was performed on the neat PGS and PGS/CNCs composites. The thermal parameters, such as, glass transition temperature (T_g) and crystallization temperature (T_c) were measured from the DSC curves. Firstly, the neat PGS and PGS/CNCs composites individually had a crystallization peak at $-18 \sim -21$°C, which revealed that they are semi-crystalline polymer beings. With the addition of CNCs, the T_c of PGS decreased monotonously from -18°C to -21°C. One possible reason is that the CNCs acted as the nucleating agents, which prompted the perfection of crystallization in PGS, subsequently improved the crystallization

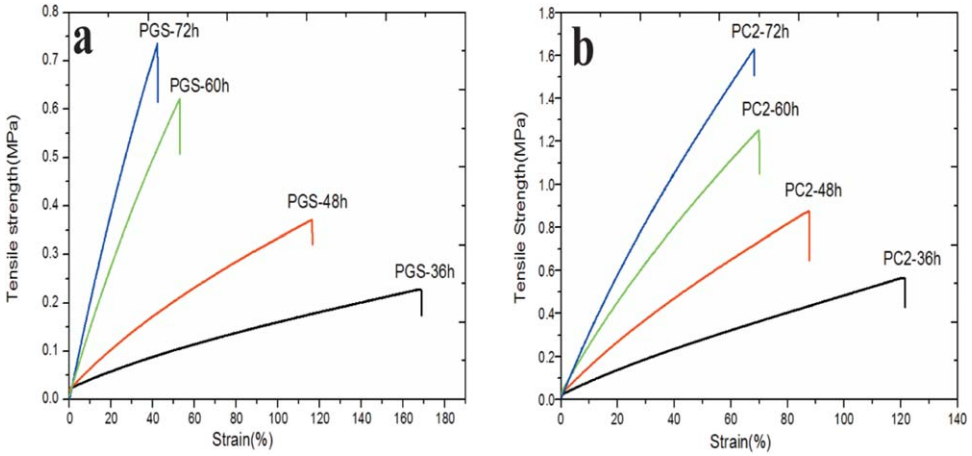

Figure 4. Tensile stress–strain curves of (a) neat PGS; (b) PC2 (PGS with 2 wt % CNCs) at different crosslinking curve times (36, 48, 60, and 72 h). [Color figure can be viewed in the online issue, which is available at wileyonlinelibrary.com.]

Table II. The Sol–Gel Content, Degree of Swelling in THF and Water Absorption and Water Contact Angle of PGS/CNCs Composites

Sample	CNCs (wt %)	Sol (wt %)	Gel (wt %)	Degree of swelling (%)	Water absorption (%)	Water contact angle (°)
PC0	0	21.2±0.4	78.8±0.4	450±17	7.2±0.5	85.7±2.0
PC1	1	16.2±0.3	83.8±0.3	325±10	9.2±0.4	74.2±1.0
PC2	2	15.7±0.3	84.3±0.3	296±20	11.2±0.3	72.6±1.0
PC3	3	13.5±0.4	86.5±0.4	233±8.0	13.4±0.4	71.7±0.8
PC4	4	13.2±0.3	86.8±0.3	219±5.0	18.6±0.6	68.1±1.2

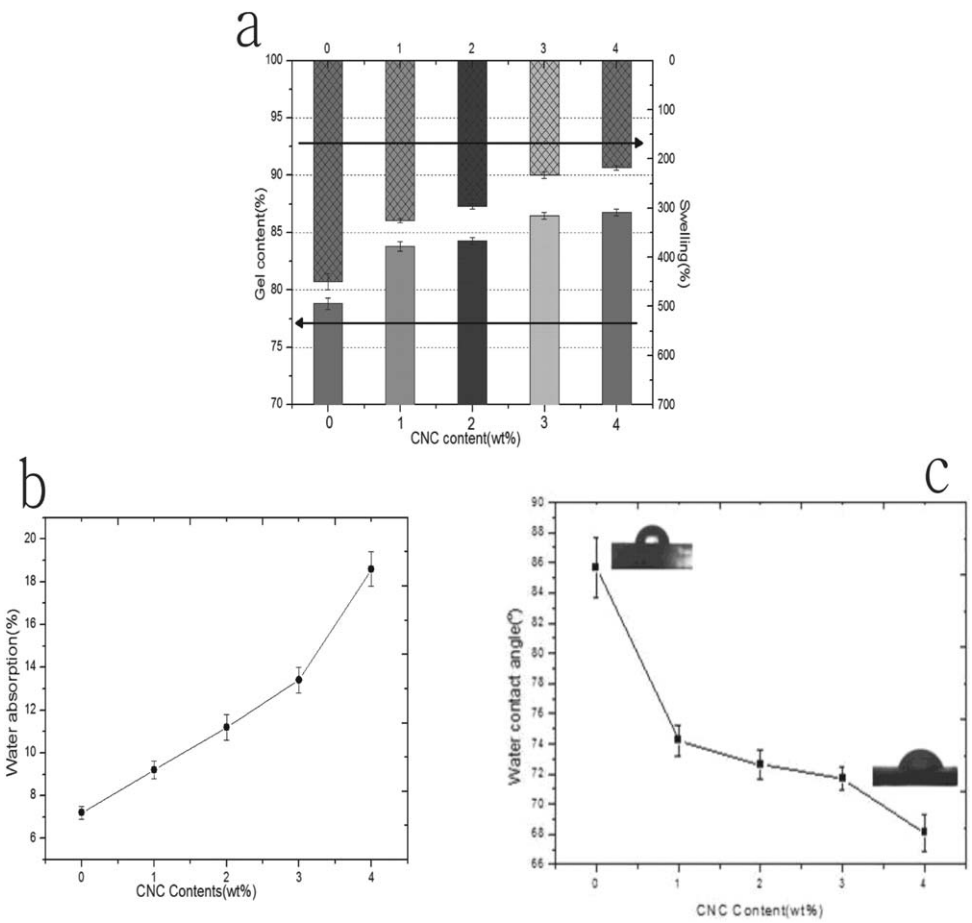

Figure 5. The crosslink density and hydrophilic properties of PGS/CNCs composites: (a) gel content and degree of swelling; (b) water absorption; (c) water contact angle.

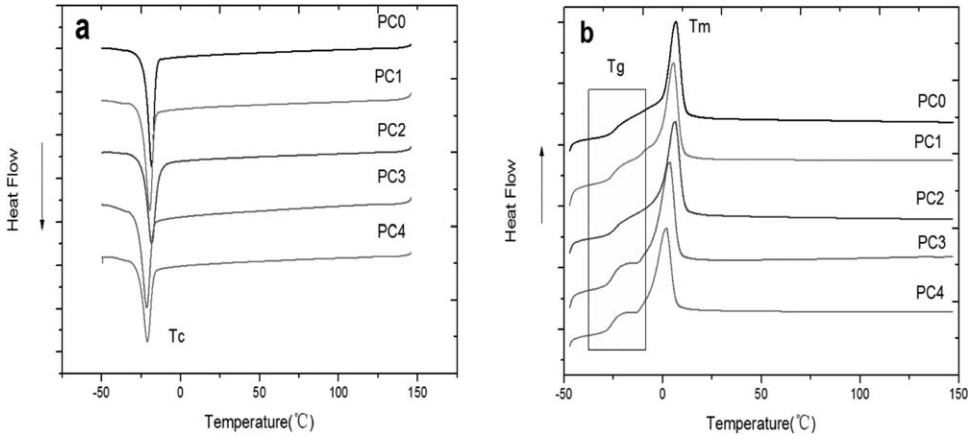

Figure 6. DSC curves of PGS composites with different CNCs loadings: PC0∼5 represent PGS with 0, 1, 2, 3, 4 wt % of CNCs.

Table III. T_g and T_c of the PGS/CNCs Composites

Sample	Glass transition temperature (T_g/°C)	Crystallization temperature (T_c/°C)
PC0	−24.5	−18.2
PC1	−24.9	−19.5
PC2	−24.2	−18.3
PC3	−25.6	−21.2
PC4	−25.9	−21.5

capacity of PGS matrix. Secondly, for T_g, it usually reflects the movement capability of polymer molecular chain segments which was mainly dependent on the interaction among the molecular chains.[17] On the whole, T_g of the composites were about −24°C lower than room temperature, demonstrating that the moving capability of molecular chain segments of the PGS matrixes was strong. The composites showed certain elasticity under room or body temperature because of the low T_g. With the increase of CNCs loadings, T_g of the composites presented a slight decrease indicated that the moving capability of polymer molecular chain was strengthened. Normally, it is well known that, the T_g of PGS will rise with the increase of crosslinking density of the matrix (shown in Table II), but actually the result was just the opposite. This was probably caused by the introduction of CNCs which weakened the intramolecular hydrogen bonding action of PGS, because the physical adsorption substituted some hydrogen bonds and hindered them from formation. Overall, the combined action strengthened the moving capability of PGS molecular chain slightly which led to only a 1.4°C difference of T_g between neat PGS and PGS with 4 wt % CNCs loadings.

In Vitro Degradation Behavior of PGS/CNCs Composites

The mass losses of the composites at different degradation periods are displayed in Figure 7. Firstly, all the composites had a monotonous mass loss with time, but still lower than 30% at the degradation period of 80 days. The similar result has been reported previously by Wang *et al.*, which indicated that the PGS film lost only 17.6% of its dry weight on day 60 under in vitro degradation condition at 37°C in PBS.[23] It demonstrated that the PGS matrix had a very slow degradation rate under *in vitro* than *in vivo* which completely absorbed the PGS within 60 days.[10] Secondly, with the addition of CNCs, the degradation rate of all the composites presented firstly an upward trend but then followed by a decrease [Figure 7(a)], which reached the highest value at the CNCs loadings of 2 wt % [Figure 7(b)]. It was supposed that the degradation rate was influenced by the addition of CNCs in two opposing manners. On the one hand, introduction of the hydrophilic CNCs could effectively accelerate the water attack in the hydrophobic PGS and thus increase the hydrolysis rate. On the other hand, the crosslink density of PGS network was also increased in the composite (Table II) due to the possible chemical reaction between PGS and CNCs, as a result, the degradation rate of material could be slowed down by the addition of CNCs. Therefore, the addition of CNCs filler could be a control of PGS degradation kinetics which offered an opportunity to achieve a satisfactory balance of degradation rate and mechanical flexibility simultaneously in the elastomeric composites.

CONCLUSIONS

In this article, it prepared and characterized PGS and PGS/CNCs composites with 1, 2, 3, and 4 wt % CNCs. As expected, the addition of CNCs greatly improved both the tensile strength (0.45 MPa to 1.5 MPa) and modulus (0.76 MPa to 1.9 MPa) of PGS while maintaining the extensibility of composites with only 4 wt % CNCs loadings. Prolonging the curing time promoted the development of crosslinked network of PGS, subsequently further improved the strength for both neat PGS and PGS/CNCs composites. DSC analysis indicated that the addition of CNCs decreased the crystallization temperature (T_c) of PGS matrix from −18.2°C to −21.5°C, while maintaining the glass transition temperature (T_g) at around −25°C. Moreover, the hydrophilic ability of PGS was also improved due to the introduction of strong hydrophilic CNCs. Degradation tests showed that the adding of CNCs tailored the degradation rate of composites, in which PGS with 2 wt % CNCs had the fastest degradation rate.

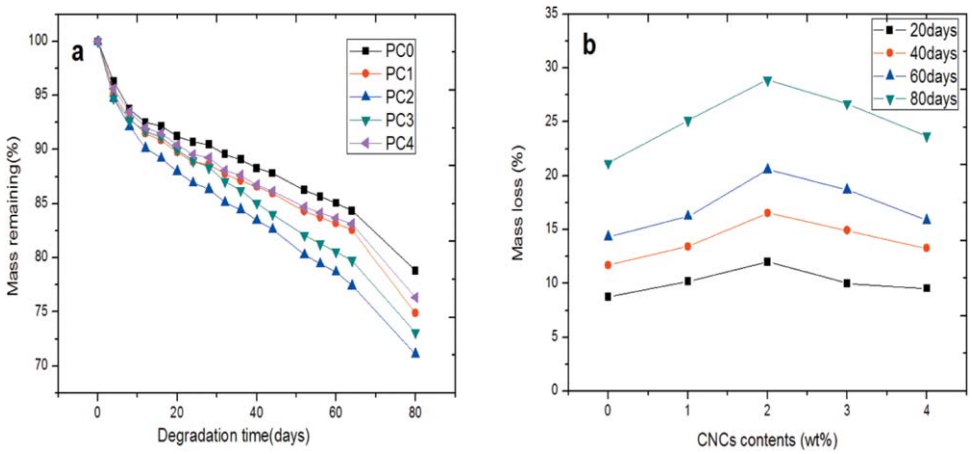

Figure 7. (a) Mass loss-degradation time curves of the PGS/CNCs composites with different loadings of CNCs; (b) Mass loss of all composites for 20, 40, 60 and 80 days. [Color figure can be viewed in the online issue, which is available at wileyonlinelibrary.com.]

ACKNOWLEDGMENTS

The authors gratefully acknowledge National Natural Science Foundation of China (U1134005/L04) for financial supports.

REFERENCES

1. Jaafar, I. H.; Ammar, M. M.; Jedlicka, S. S.; Pearson, R. A.; Coulter, J. P. *J. Mater. Sci.* **2010**, *45*, 2525.
2. Freed, L. E.; Engelmayr, G. C.; Borenstein, J. T.; Moutos, F. T.; Guilak, F. *Adv. Mater.* **2009**, *21*, 3410.
3. Zaky, S. H.; Hangadora, C. K.; Tudares, M. A.; Gao, J.; Jensen, A.; Wang, Y.; Almarza, A. J. *Biomed. Mater.* **2014**, *9*, 025003.
4. Ravichandran, R.; Venugopal, J. R.; Sundarrajan, S.; Mukherjee, S.; Ramakrishna, S. *Tissue. Eng. Part. A* **2011**, *17*, 1363.
5. Rai, R.; Tallawi, M.; Barbani, N.; Frati, C.; Madeddu, D.; Cavalli, S.; Boccaccini, A. R. *Mater. Sci. Eng: C* **2013**, *33*, 3677.
6. Bodakhe, S.; Verma, S.; Garkhal, K.; Samal, S. K.; Sharma, S. S.; Kumar, N. *Nanomedicine* **2013**, *8*, 1777.
7. Bruggeman, J. P.; Bettinger, C. J.; Nijst, C. L.; Kohane, D. S.; Langer, R. *Adv. Mater.* **2008**, 20, 1922.
8. Woodruff, M. A.; Hutmacher, D. W. *Prog. Polym. Sci.* **2010**, *35*, 1217.
9. Liang, S. L.; Cook, W. D.; Thouas, G. A.; Chen, Q. Z. *Biomaterials* **2010**, *31*, 8516.
10. Rai, R.; Tallawi, M.; Grigore, A.; Boccaccini, A. R. *Prog. Polym. Sci.* **2012**, *37*, 1051.
11. Rai, R.; Tallawi, M.; Roether, J. A.; Detsch, R.; Barbani, N.; Rosellini, E.; Boccaccini, A. R. *Mater. Lett.* **2013**, *105*, 32.
12. Pereira, M. J. N.; Ouyang, B.; Sundback, C. A.; Lang, N.; Friehs, I.; Mureli, S.; Karp, J. M. *Adv. Mater.* **2013**, *25*, 1209.
13. Chen, Q. Z.; Bismarck, A.; Hansen, U.; Junaid, S.; Tran, M. Q.; Harding, S. E.; Boccaccini, A. R. *Biomaterials* **2008**, *29*, 47.
14. Li, Y.; Cook, W. D.; Moorhoff, C.; Huang, W. C.; Chen, Q. Z. *Polym. Int.* **2013**, *62*, 534.
15. Wu, Y.; Shi, R.; Chen, D.; Zhang, L.; Tian, W. *J. Appl. Polym. Sci.* **2012**, *123*, 1612.
16. Chen, Q. Z.; Liang, S. L.; Wang, J.; Simon, G. P. *J. Mech. Behav. Biomed. Mater.* **2011**, *4*, 1805.
17. Liu, Q. Y.; Wu, J.; Tan, T.; Zhang, L.; Chen, D.; Tian, W. *Polym. Degrad. Stabil.* **2009**, *94*, 1427.
18. Dufresne, A. *Mater. Today* **2013**, *16*, 220.
19. Kamphunthong, W.; Hornsby, P.; Sirisinha, K. *J. Appl. Polym. Sci.* **2012**, *125*, 1642.
20. Fortunati, E.; Puglia, D.; Monti, M.; Santulli, C.; Maniruzzaman, M.; Kenny, J. M. *J. Appl. Polym. Sci.* **2012**, *128*, 1320.
21. Siró, I.; Plackett, D. *Cellulose* **2010**, *17*, 459.
22. Wu, T.; Frydrych, M.; O'Kelly, K.; Chen, B. *Biomacromolecules* **2014**, *15*, 2663.
23. Wang, Y. D.; Ameer, G. A.; Sheppard, B. J.; Langer, R. *Nat. Biotechnol.* **2002**, *20*, 602.
24. Kharaziha, M.; Nikkhah, M.; Shin, S. R.; Annabi, N.; Masoumi, N.; Gaharwar, A. K.; Khademhosseini, A. *Biomaterials* **2013**, *34*, 6355.
25. Coleman, M. M.; Skrovanek, D. J.; Hu, J.; Painter, P. C. *Macromolecules* **1988**, *21*, 59.
26. Kemppainen, J. M.; Hollister, S. J. *J. Biomed. Mater. Res: A.* **2010**, *94*, 9.
27. Liu, Q.; Tian, M.; Shi, R.; Zhang, L.; Chen, D.; Tian, W. *J. Appl. Polym. Sci.* **2007**, *104*, 1131.
28. Mitsak, A. G.; Dunn, A. M.; Hollister, S. J. *J. Mech. Behav. Biomed. Mater.* **2012**, *11*, 3.
29. Li, Y.; Huang, W.; Cook, W. D.; Chen, Q. Z. *Biomed. Mater.* **2013**, *8*, 035006.
30. Kafouris, D.; Kossivas, F.; Constantinides, C.; Nguyen, N. Q.; Wesdemiotis, C.; Patrickios, C. S. *Macromolecules* **2013**, *46*, 622.